Dual inhibition of sodium-mediated proton and calcium efflux triggers non-apoptotic cell death in malignant gliomas

William Harley , Candace Floyd , Tamara Dunn , Xiao-Dong Zhang , Tsung-Yu Chen , Manu Hegde , Hasan Palandoken , Michael H. Nantz , Leonardo Leon , K.L. Carraway III , Bruce Lyeth , Fredric A. Gorin

A B S T R A C T

Malignant glioma cells maintain an elevated intracellular pH (pH_i) within hypoxic ischemic tumor microenvironments through persistent activation of sodium proton transport (McLean et al., 2000). Amiloride has been reported to selectively kill human malignant glioma cell lines but not primary astrocytes (Hegde et al., 2004). While amiloride reduces pH_i of malignant gliomas by inhibiting isoform 1 of sodium proton exchange (NHE1), direct acidification was shown to be cytostatic rather than cytotoxic. At cytotoxic concentrations, amiloride has multiple drug targets including inhibition of NHE1 and sodium calcium exchange. Amiloride's glioma cytotoxicity can be explained, at least in part, by dual inhibition of NHE1 and of Na^+ dependent calcium efflux by isoform 1.1 of the sodium calcium exchanger (NCX1.1) , which increases $[Ca^{2+}]_i$ and initiates glioma cell demise. As a result of persistent NHE1 activity, cytosolic free levels of sodium ($[Na^+]_i$) in U87 and C6 glioma cells are elevated 3 fold, as compared with normal astrocytes. Basal cytosolic free calcium levels ($[Ca^{2+}]_i$) also are increased 5 fold. 2′, 4′ dichlorobenzamil (DCB) inhibits the sodium dependent calcium transporter (NCX1.1) much more potently than NHE1. DCB was employed in a concentration dependent fashion in glioma cells to selectively inhibit the forward mode of NCX1.1 at ≤ 1 μM, while dually inhibiting both NHE1 and NCX1.1 at ≥ 20 μM. DCB (1 μM) was not cytotoxic to glioma cells, while DCB (20 μM) further increased basal elevated levels of $[Ca^{2+}]_i$ in glioma cells that was followed by cell demise. Cariporide and SEA0400 are more selective inhibitors of NHE1 and NCX1.1 than amiloride or DCB, respectively. Individually, Cariporide and SEA0400 are not cytotoxic, but in combination induced glioma cell death. Like amiloride, the combination of Cariporide and SEA0400 produced glioma cell death in the absence of demonstrable caspase activation.

1. Introduction

Malignant gliomas (WHO grades 3 and 4) are the most prevalent primary adult brain tumors with a recurrence rate exceeding 90% within two years following conventional therapeutic modalities (Legler et al., 1999; Brandes et al., 1999). These rapidly proliferating and infiltrating primary astroglial cancers outgrow their neovascularization induced by vasogenic endothelial growth factor (VEGF) and create hypoxic ischemic tumor domains containing necrotic glioma cells bordered by non proliferating, pseudopallisading glioma cells and proliferating glioma cells (Gorin et al., 2004). Glioma necrosis remains one of the most consistent pathological features predictive of glioma recurrence and a worsened clinical prognosis (Brandes et al., 1999; Compostella et al., 2007). We and others reported that glioma cells survive and proliferate within these hypoxic ischemic tumor microenvir onments (Gorin et al., 2004; Korkolopoulou et al., 2007). The resultant extracellular acidosis in hypoxic ischemic tumor microenvironments is associated with glioma cell cycle arrest. We found that acidified glioma cells having high levels of nuclear cyclin D1 enter cell cycle arrest at external pH (pH_{ext}) 6.0, are capable of surviving prolonged acidosis, and resume proliferation when the pH_{ext} of the tumor microenvironment is normalized (Schnier et al., 2008). Not surprisingly, hypoxic ischemic glioma cells are reported to possess increased resis tance to radiation therapy and alkylating agents such as BCNU and temozolomide (Barker et al., 1996; Vaupel and Mayer, 2007; Dinca et al., 2007). Recent clinical experience treating malignant gliomas with bevacizumab indicates that anti VEGF therapy is cytostatic and can be followed by the recurrence of disseminated glioma initiating cells (Chamberlain and Johnston, 2009; Lamszus et al., 2003). Therefore, it is necessary to investigate new cytotoxic agents targeting these glioma initiating cells. Amiloride, an FDA approved diuretic, is cytotoxic to glioma cells in the micromolar range and previously reported to be non toxic to primary astrocytes (Hegde et al., 2004). In vivo, amiloride has been identified as killing proliferating and non proliferating perine crotic glioma cells in perinecrotic regions in an immunodeficient murine intracerebral human U87 glioma xenograft model (Gorin, 2007).

Surprisingly, ^{31}P NMR studies in individuals with WHO grade 3 and 4 gliomas reported normocidic or elevated pH_{tot} within the tumors despite their increased glycolytic fluxes (Maintz et al., 2002). We have measured the pH_i of several malignant glioma cell lines, including human U87, U251, U118 and murine C6, and determined that all these glioma cell lines maintain an alkalotic pH_i between 7.2 and 7.4 in a bicarbonate depleted environment (McLean et al., 2000). Their intracellular alkalosis is a conse quence of persistent activity of NHE1, which maintains an elevated intracellular pH optimized for non oxidative glycolysis in these highly metabolically active cancers (Gorin et al., 2004; Griguer et al., 2005). Inhibiting NHE1 in human malignant glioma cell lines in bicarbonate free media reduced their elevated pH_i to that of normal astrocytes (6.9 7.0) (McLean et al., 2000). By contrast, astrocytes do not activate NHE1 while maintaining pH_i of 6.9 7.0 in the normal brain milieu and are not acidified by NHE1 inhibition (McLean et al., 2000). Astrocytes and glioma cell lines additionally express NCX1.1 and acid sensing ion channels (ASICs) (Goldman et al., 1994; Amoroso et al., 1997; Vila Carriles et al., 2006). ASIC1a generates constitutive inward sodium and calcium currents in several glioma cell lines thought to enhance proliferation and mobility, but not alter their viability (Vila Carriles et al., 2006).

Both NHE1 and ASIC1a are blocked by amiloride, and it has been proposed that amiloride selectively kills specific cancer cell types by reducing their pH_i and thereby inhibiting non oxidative glycolysis (Tannock and Rotin, 1989; Reichert et al., 2002; Wu et al., 2007). However, neither acidifying U87 or U118 glioma cell lines to pH_i 6.9 by bathing them in reduced pH media (6.8) or selectively inhibiting NHE1 with Cariporide (HOE642), was cytotoxic (Hegde et al., 2004). Cariporide inhibits NHE1 with an IC_{50} of 26 nM (Masereel et al., 2003), and in contrast to amiloride, has not been shown to inhibit ASICs or NCX1.1. The concentration range of amiloride (100 500 μM) capable of selectively killing either proliferating (pH_{ext} 7.0) or non proliferating human malignant glioma cell lines (pH_{ext} 6.0), while remaining non toxic to normal brain cell types, indicates that further study of its cytotoxic mechanisms of action could lead to the development of more potent anti cancer agents.

An important physiological consequence of persistent NHE1 activity in glioma cells would be an anticipated increase in $[Na^+]_i$; consistent with the depolarized membrane poten tials reported in the human U87 glioma cell line (48 to + 15 mV) (Ducret et al., 2003). This magnitude of depolarization in glioma cells, as compared with normal astrocytes (80 mV) (Perez Velazquez et al., 1996), is predicted to increase intracellular calcium influx via voltage activated plasmalem mal channels and sodium dependent calcium transport mechanisms, as we reported in stretch injured astrocytes (Floyd et al., 2005) and others have described in hypoxic cardiomyocytes following reperfusion injury (Wang et al., 2007). However, the specific cellular mechanisms underlying the calcium loading of depolarized malignant glioma cells is beyond the scope of this investigation which is focused upon amiloride induced glioma demise.

In this study, we demonstrate that malignant glioma cells maintain elevated levels of $[Na^+]_i$ and $[Ca^{2+}]_i$ in comparison to normal astrocytes. These ionic alterations could explain the selective killing of glioma cells by amiloride at concentrations that inhibit Na^+ dependent H^+ efflux by NHE1 and Na^+ dependent Ca^{2+} efflux ("forward mode") by NCX1.1, further elevating $[Ca^{2+}]_i$ to cytotoxic levels. Selective pharmacological inhibition of either NCX1.1 or NHE1 is not cytotoxic to glioma cells. However, dual inhibition of NHE1 and the forward mode of NCX1.1 further elevate $[Ca^{2+}]_i$ and precede observed glioma cell demise. A summary diagram of the ionic transporters, intracellular calcium stores, and pharmacological agents evaluated in this study is summarized in Fig. 1.

2. Results

2.1. *Intracellular levels of cytosolic free sodium are elevated in glioma cells*

Initial basal concentrations of cytosolic free sodium $[Na^+]_i$ are 3 to 3.5 fold higher in U87 and C6 glioma cells, respectively, as compared with primary astrocytes (Fig. 2). Addition of the non

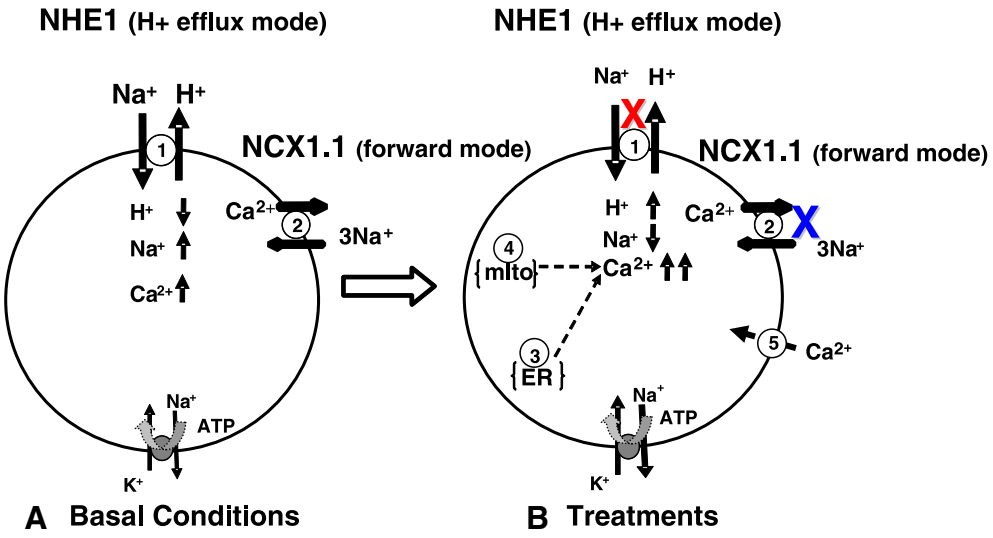

Fig. 1 – Panel A: Basal conditions of sodium-mediated exchangers and intracellular calcium stores in glioma cells. Panel B: {1} Inhibition of sodium-mediated proton exchange (NHE1) by Cariporide. {2} Inhibition of sodium-mediated calcium exchange (NCX1.1) by dichlorobenzamil (1 μM DCB) or SEA0400. {1} and {2} Dual inhibition of NHE1 and NCX1.1 by either amiloride, DCB (20 μM), Cariporide + DCB (1 μM), or Cariporide + SEA0400. {3} Release of calcium from endoplasmic reticulum by thapsigargin (TG). {4} Release of calcium from mitochondria by carbonyl cyanide p-trifluoromethoxyphenyl hydrazone (FCCP). {5} Extracellular calcium entry by the ionophore, ionomycin. See text for experimental details.

fluorescent, reversible NHE1 inhibitor HOE694 to either of these two glioma cell lines (Figs. 2A, B) reduced $[Na^+]_i$ at time 0 to concentrations comparable to that of astrocytes (~10 mM, Fig. 2C). Replacement of buffer without HOE694 at 5 min increased $[Na^+]_i$ to their initially elevated basal levels of 32 mM ± 2 within 20 60 min. These NHE1 inhibitor studies demonstrate that in a bicarbonate free environment, elevated $[Na^+]_i$ in glioma cells is primarily a consequence of persistent NHE1 activity that is associated with their elevated pH_i (Fig. 1, panel A).

2.2. *Intracellular levels of free calcium are elevated in glioma cells*

Basal levels of cytosolic free calcium $[Ca^{2+}]_i$ of 400 nM and are 5 fold higher in U87 glioma cells, as compared with primary astrocytes, in which we reported a $[Ca^{2+}]_i$ of 80 nM (Fig. 3A) (Floyd et al., 2005). Elevated basal levels of cytosolic free calcium in U87 glioma cells were not altered by reduced glioma cell pH_i from 7.4 to 6.9 with acidified HEPES media of pH_{ext} 6.8 (Hegde et al., 2004), or by inhibiting NHE1 with non fluorescent HOE694 (Fig. 3A). Therefore elevated levels of $[Ca^{2+}]_i$ in glioma cells, unlike $[Na^+]_i$, are not directly coupled to persistent NHE1 activity.

2.3. *Further elevation of cytosolic free calcium in glioma cells using a calcium ionophore produces glioma cell death*

Ionomycin is a bacterial ionophore that increases calcium influx through the plasmalemma. The addition of 5 μM ionomycin rapidly increased levels of cytosolic free calcium released from intracellular stores by thapsigargin (TG) (Fig. 3B). Ionomycin (5 μM) killed 54 ± 7% of U87 glioma cells at 24 h, as compared with time matched controls, based upon the manual trypan blue exclusion assay to count dead cells. Using the WST assay to measure metabolically active cells, only 27 ± 2% of glioma cells were viable, compared with controls. The ionomycin experiments demonstrated that directly increasing levels of free cytosolic calcium by increas ing calcium influx produced glioma cell demise.

2.4. *Intracellular calcium buffering and calcium efflux*

The insensitivity of elevated $[Ca^{2+}]_i$ to NHE1 activity is not unexpected, given the calcium buffering by intracellular stores and calcium efflux mechanisms previously demonstrated in glioma cells and normal astrocytes (Floyd et al., 2005; Galiano et al., 2004). Thapsigargin (TG) inhibits calcium ATPase to release calcium from TG sensitive stores in the endoplasmic reticulum. Incubating U87 glioma cells and astrocytes with TG (1 μM) caused calcium release from ER stores, reflected by an increase in cytosolic calcium (Fig. 3C). A significant amount of cytosolic free calcium is released by TG sensitive ER stores in glioma cells, as compared with astrocytes. Calcium release from ER stores was consistently observed in gliomas but not astrocytes. However, quantification of subsequent cytosolic free calcium concentrations, even with loading of low affinity Fura FF, was hampered, in part by variable activation of store operated calcium entry throughout the polyploid glioma cell populations (Spassova et al., 2004; Kwan et al., 2008). Importantly, $[Ca^{2+}]_i$ released from ER stores additionally increased the already elevated levels of cytosolic free calcium, which returned to basal levels within 400 s (Fig. 3C).

FCCP (carbonyl cyanide p trifluoromethoxyphenyl hydra zone) collapses the mitochondrial transmembrane potential

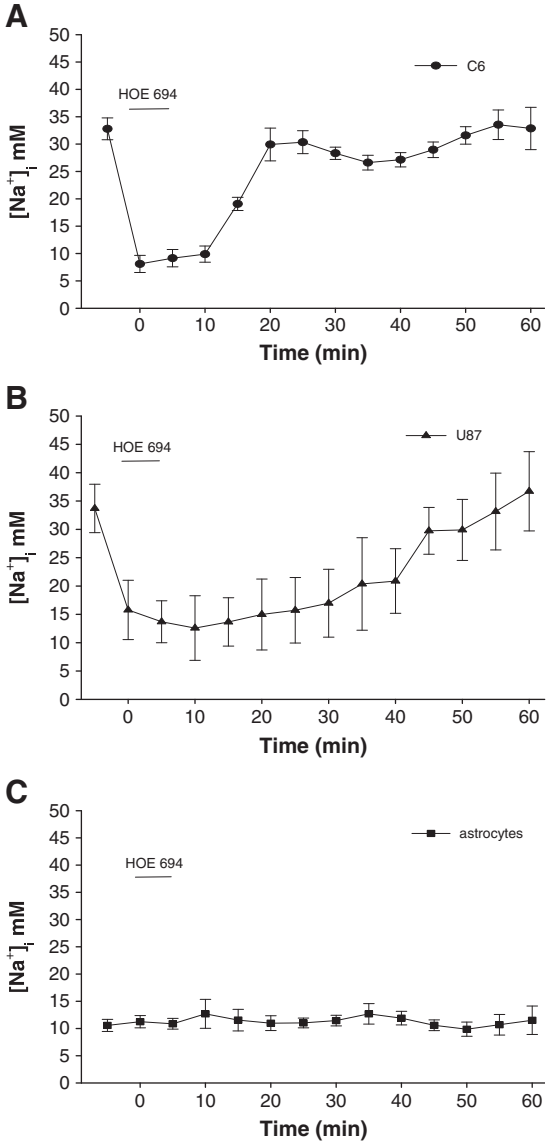

Fig. 2 – Intracellular cytosolic free sodium concentrations in two glioma cell lines (A) C6 and (B) U87, and (C) primary rat astrocytes treated with a reversible, non-fluorescent NHE1 inhibitor, HOE694 (100 μM), at time 0 for 5 min followed by washout. The first data point in each graph represents basal $[Na^+]_i$ for each cell type.

(ψ_m) causing the release of calcium from mitochondrial stores (Vali et al., 2000; Chalmers and Nicholls, 2003). In normal astrocytes and other normal cell types, collapse of the trans membrane mitochondrial potential does not demonstrably increase $[Ca^{2+}]_i$ (Kahlert et al., 2001). In U87 glioma cells, FCCP caused a large increase in $[Ca^{2+}]_i$ and a negligible $[Ca^{2+}]_i$ increase in normal astrocytes (Fig. 3C). Like TG, FCCP induced increase in $[Ca^{2+}]_i$ was transient and returned to near basal levels.

2.5. *Sodium-dependent calcium efflux by NCX1.1 is inhibited selectively by DCB*

DCB is an amiloride analog whose C2 dichloroaryl side chain greatly enhances its inhibition of NCX1.1 ≫ NHE1, and DCB is widely employed as an inhibitor of sodium mediated calcium transport. Glioma cells and astrocytes express NCX1.1, there fore it is necessary to examine the concentration dependent inhibition of the forward and reverse modes of NCX1.1 stably transfected into Chinese hamster ovary (CHO) cells. CHO cells lack the ion transporters and calcium channels that partici pate in the glutamate glutamine cycle of astroglial cell types and which confound measurements of sodium calcium transport in glioma cells (Ishiuchi et al., 2007; Handfield Jones et al., 1988; Deitmer et al., 2003). Whole cell patch electrophysiological recordings of CHO cells stably transfected with NCX1.1 demonstrate an IC_{50} of 9 nM for DCB to prevent sodium dependent calcium efflux ("forward mode", Fig. 4A). Furthermore, these whole patch studies demonstrate that DCB is a much less effective inhibitor of sodium dependent calcium influx ("reverse mode") by NCX1.1 (IC_{50} 22 μM, Fig. 4B). These electrophysiological findings permitted us to employ low concentrations of DCB (≤1 μM) to selectively block the forward mode of NCX1.1. Compounds such as SEA0400 can be employed to preferentially block the reverse mode of NCX1.1 with nanomolar potencies under the observed glioma condi tions of elevated $[Na^+]_i$ (Iwamoto, 2004). Higher concentrations of DCB (≥20 μM) were employed to inhibit NHE1 (Hegde et al., 2004), the forward mode of NCX1.1, and partially inhibit the reverse mode of NCX1.1 (Fig. 1, panel B).

2.6. *Inhibition of the forward mode of NCX1.1 by low concentration DCB maintains elevated Ca_i^+ following release from intracellular stores, but does not initiate glioma cell death*

The objective of the following studies was to determine whether the transient increase in levels of cytosolic calcium released from intracellular stores was being moderated by the forward mode of NCX1.1. DCB (1 μM) was added 90 100 s prior to the addition of thapsigargin so that there was an insufficient time for inhibition of the forward mode of NCX1.1 to increase basal levels of cytosolic free calcium prior to the addition of TG. DCB (1 μM) prevented the restoration of $[Ca^{2+}]_i$ to basal elevated levels in U87 glioma cells following release from ER stores with TG (Fig. 3C). Significantly, DCB (1 μM) was not cytotoxic to glioma cells nor was SEA0400 (1 μM), which preferentially blocks the reverse mode of NCX1.1 with an IC_{50} of 78 nM in the presence of elevated $[Na^+]_i$ (Table 1) (Lee et al., 2004). Inhibition of NCX1.1 by 1 μM DCB did not significantly increase glioma cell death (Table 1, % trypan blue), as compared with time matched, vehicle treated con trols. However, low concentration DCB was observed to possess a modest anti proliferative effect as determined by the WST assay (% viable cells < (100 % dead cells)) (Table 1).

2.7. *Inhibition of NHE1 by Cariporide does not initiate glioma cell death while dual inhibition of NCX1.1 and NHE1 by DCB produces caspase-independent glioma cell death*

The objective of the following studies was to determine whether dual inhibition of NHE1 and NCX1.1 contributed to amiloride's cytotoxic effects, as measured using the trypan blue exclusion assay. Additionally, the viabilities of treated cells, as compared with time matched controls, were measured using the WST tetrazolium assay to assess whether any of these agents had

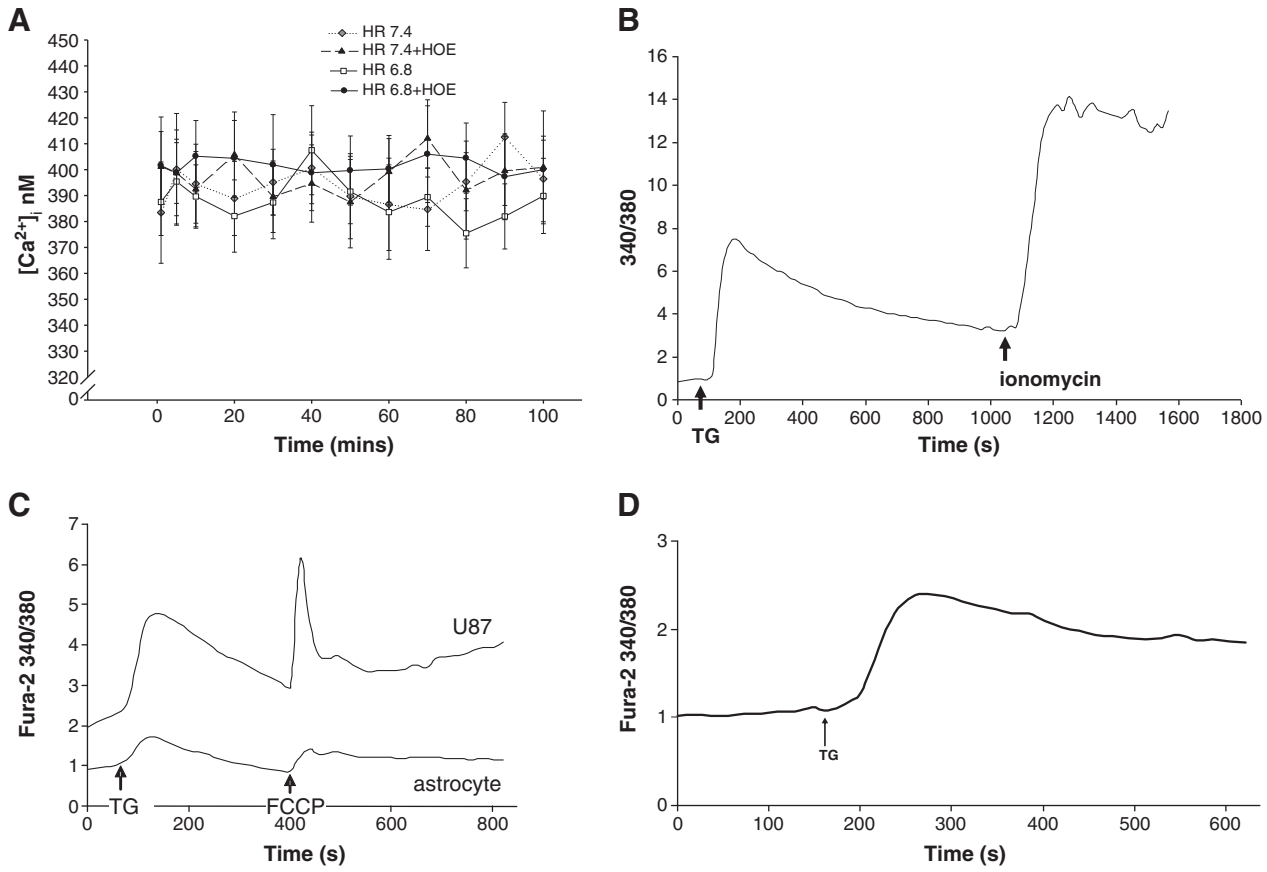

Fig. 3 – (A) Levels of cytosolic free calcium $[Ca^{2+}]_i$ in U87 glioma cells maintained at pH_{ext} 7.4 or 6.8 in the presence or absence of the NHE inhibitor HOE 694 (100 μM). Basal $[Ca^{2+}]_i$ in astrocytes is between 50 and 80 nM as previously reported [26]. (B) Thapsigargin (TG) followed by ionomycin-induced 340/380 ratio changes in U87 glioma cells loaded with Fura-2. TG initiated calcium release from ER while the ionophore, ionomycin by increased calcium influx and produced a larger and persistent elevation in the 340/380 ratio. (C) Thapsigargin (TG) and FCCP-induced 340/380 ratio changes in primary rat astrocytes and in U87 glioma cells loaded with Fura-2. TG or FCCP triggered calcium release in glioma cells from the ER or mitochondria, respectively, as evidenced by an initial 2-fold increase in the 340/380 ratio in a representative study. A modest increase in the 340/380 ratios was observed in primary astrocytes following these treatments. Upper and lower lines represent a typical experiment with U87 glioma cells or primary astrocytes, respectively. (D) Persistent elevation of the 340/380 ratio of Fura-2 in U87 cells pretreated with DCB (1 μM) 90 s prior to the addition of thapsigargin (10 μM). DCB (1 μM) blocked sodium-dependent calcium efflux ("forward mode") of NCX1.1 in U87 glioma cells to prevent moderation of elevated cytosolic calcium shown in B and C.

significant cytostatic activities independent of their cytotoxic activities. U87 glioma cell death and total live cell numbers were not affected by NHE1 inhibition by Cariporide (HOE642); a more stable NHE1 inhibitor than the non fluorescent HOE694 used for the fluorescence studies (Table 1). At higher concentrations of DCB (20 μM) there was a marked 4 fold increase in glioma cell death and a significant decrease in viable cells (Table 1). Amiloride or 20 μM DCB demonstrated comparable cytotoxicities when tested in U87, U251 and U118 human glioma cell lines (Table 1). Previously, all three human cell lines had been shown by us to maintain elevated pH_i resulting from persistent activation of NHE1 (McLean et al., 2000).

2.8. *Treatment with both SEA400 and Cariporide or DCB and Cariporide produces caspase-independent glioma cell death*

The amiloride and DCB cytotoxicity data suggested that dual inhibition of NHE1 and the forward mode of NCX1.1 maintained elevated $[Ca^{2+}]_i$. Low concentration DCB (1 μM) combined with 100 μM Cariporide killed 39±4% of U87 glioma cells after 48 h when compared with time matched controls (Table 1). A similar number of viable cells (35±3%) were detected following this treatment using the WST live cell assay. The magnitude of glioma cell death produced by 100 μM Cariporide+1 μM DCB were not altered by pre incubation with the pan caspase inhibitor zVAD.FMK (34+/ 2%).

Both amiloride and DCB reportedly inhibit ASIC2A at higher concentrations (Page et al., 2007), so that it was useful to employ other agents that inhibited either NHE1 (Cariporide) or NCX1.1 (SEA0400), but did not inhibit ASIC. Neither Cariporide nor SEA0400 individually caused glioma cell death, but in combination they were cytotoxic to glioma cells (Table 1). The cytotoxic effects of Cariporide+SEA0400 were not affected by pre incubation with the pan caspase inhibitor zVAD.FMK (Table 1).

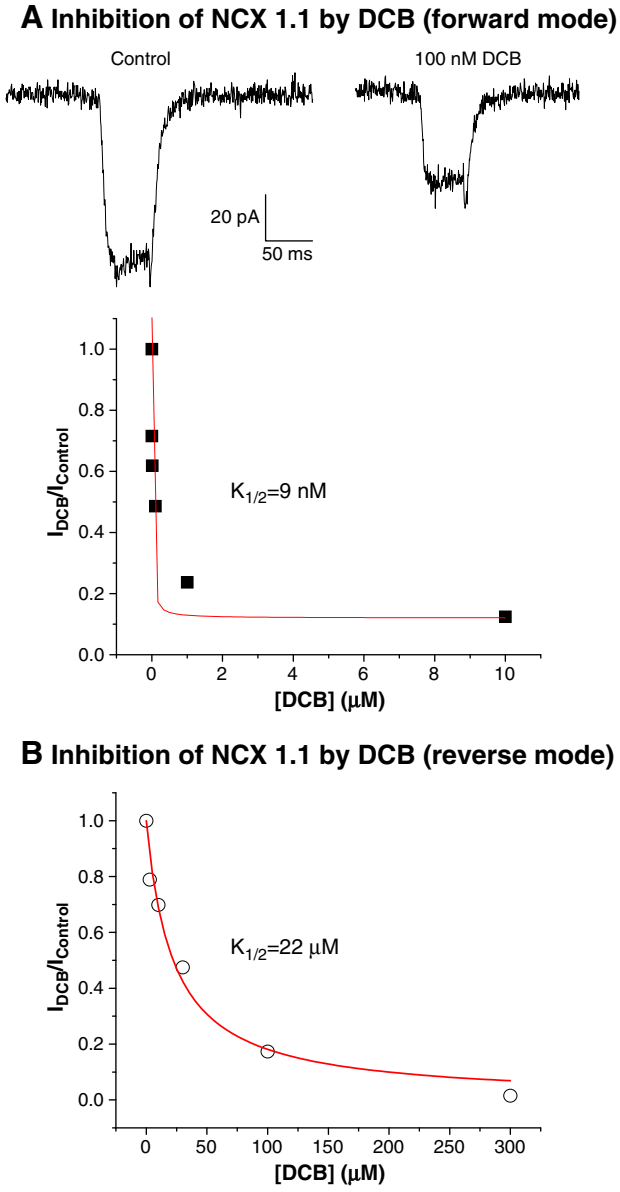

Fig. 4 – Representative whole-cell voltage clamp data used to determine the IC_{50} for inhibition of NCX1.1 by DCB. The graph depicts the data plot and the curve-fit line calculated used to determine the IC_{50} for inhibition of both the (A) forward and (B) reverse modes of NCX1.1.

2.9. *Treatment with Amiloride or DCB kills glioma cells without increased caspase activation and produces nuclear morphology inconsistent with apoptosis*

Immunoblot analyses showed that treatment of normal primary astrocytes or U87 glioma cells with amiloride (250 μM) or DCB (20 μM) did not significantly increase activation of caspases 3 or 7 (Fig. 5). As a positive control for apoptosis, Staurosporine (10 μM) activated caspase 7 in astrocytes and U87 glioma cells, while activating caspase 3 in glioma cells. Treating glioma cells with either amiloride or 20 μM DCB, while cytotoxic, did not produce typical apoptotic changes in nuclear morphology in U87 glioma cells stained with Hoechst 33342. Staurosporine treatment, as a positive control, produced the expected morphologic changes observed in apoptotic cells (Fig. 1S).

3. Discussion

In this study, $[Na^+]_i$ is elevated more than 3 fold in U87 and C6 glioma cells as compared with normal astrocytes. This marked elevation in $[Na^+]_i$ appears to primarily depend upon persistent NHE1 activity and is sufficient to depolarize glioma cells in hypoxic ischemic tumor regions where Na/K ATPase activity is limited by non oxidative glycolysis (Gorin et al., 2004; Erecinska et al., 1993). These ionic measurements are consistent with reported U87 glioma membrane potentials of (48 to +15 mV) (Ducret et al., 2003), as compared with 78 mV recorded in normal astrocytes (Perez Velazquez et al., 1996). This magnitude of depolarization is sufficient to increase $[Ca^{2+}]_i$ in glioma cells as a consequence of activating voltage dependent calcium channels, calcium dependent, store operated channels (SOC) (Hartmann and Verkhratsky, 1998; Kovacs et al., 2005), and can activate calcium loading by reversal of the sodium calcium transport (NCX 1.1), as we reported in stretch injured, depolarized astrocytes (Floyd et al., 2005). Here, we identified that $[Ca^{2+}]_i$ is increased by more than 5 fold and associated with elevated $[Na^+]_i$ in U87 glioma cells as compared with normal astrocytes. The ionic imbalances identified in malignant glioma cells in a bicarbonate depleted environment present an opportunity for novel drug targeting strategies by analyzing the cytotoxic consequences of markedly augmented $[Na^+]_i$ and $[Ca^{2+}]_i$ in glioma cells.

We evaluated a mechanistic model where persistently elevated cytosolic calcium in glioma cells is buffered by the endoplasmic reticulum and mitochondria and additional increases in cytosolic calcium are moderated by sodium dependent calcium efflux through NCX1.1 (Fig. 1, panel A). Ionomycin, a bacterial ionophore, produces a much greater and persistent increase in cytosolic calcium when compared with increased $[Ca^{2+}]_i$ released from the ER by thapsigargin in the same cell population (Fig. 3B). Direct glioma cytotoxicity by ionomycin appears to arise by overwhelming intracellular calcium buffering and sodium mediated calcium efflux by NCX 1.1 (Fig. 1, panel B). Inhibiting NHE1 with the reversible non fluorescent inhibitor, HOE694, reduced $[Na^+]_i$, but did not demonstrably alter elevated levels of $[Ca^{2+}]_i$ because of (1) intracellular calcium buffering and (2) sodium dependent calcium extrusion by NCX1.1 forward transport. Increased intracellular calcium buffering by the ER in glioma cells is demonstrated by the increased release of cytosolic free calcium from TG sensitive ER stores in glioma cells, as compared with astrocytes. Similarly, increased mitochondrial calcium buffering in glioma cells is shown by increased cytosolic free calcium following collapse of the transmitochondrial membrane potential (ψ_m) using FCCP. Mitochondria of several glioblastoma cell lines have been reported to sequester millimolar quantities of $[Ca^{2+}]_i$ (Hartmann and Verkhratsky, 1998). In contrast, normal primary astrocytes have 5 fold lower levels of $[Ca^{2+}]_i$ than the U87 and C6 glioma cells, and do not demonstrate an observable increase in cytosolic free calcium following mitochondrial depolarization.

Table 1 Treatment summary of cytotoxicities and cell viabilities for human malignant glioma cell lines. Cell death is expressed as a percentage of trypan blue positive cells per total cell count. Viable cell number is expressed as a percentage of the absorbance compared with time-matched, untreated controls utilizing a tetrazolium-based live cell assay (WST), which was standardized to cell number for each cell line. Asterisks (*) or (**) indicates statistical significance at $p < 0.05$ or $p < 0.005$, respectively. Abbreviations: NHE1: sodium proton exchanger, isoform 1; NCX1: sodium calcium exchanger, isoform 1.1.

Treatment after 48 h	Inhibition		U87		U251		U118	
	NHE	NCX	Cell death (SE)	Viable cells (SE)	Cell death (SE)	Viable cells (SE)	Cell death (SE)	Viable cells (SE)
Control			3 (0.32)	100 (2.3)	6 (1.5)	100 (0.89)	5 (2.1)	100 (1.9)
Dual NHE1+NCX inhibitors								
Amiloride (500 μM)	+	+	47** (2.7)	16** (3.3)	56** (4.1)	28** (2.3)	63** (5.2)	28** (4.6)
DCB (20 μM)	+	+	22** (2.1)	12** (0.9)	34** (3.6)	38** (1.7)	44** (2.7)	37** (1.1)
NCX inhibitor								
DCB (1 μM)		+	6 (1.5)	89* (1.2)	8 (1.9)	95 (0.76)	11 (3.8)	81* (5.1)
SEA400 (1 μM)		+	5 (0.86)	96 (2.2)	2 (1.5)	95 (3.2)	3 (2.2)	102 (1.9)
NHE1 inhibitor								
Cariporide (100 μM)	+		2 (0.43)	102 (1.6)	4 (0.59)	98 (2.8)	4 (1.2)	99 (3.8)
NHE1+NCX inhibitor								
Cariporide (100 μM)+DCB (1 μM)	+	+	39** (4.2)	35** (3.0)				
Cariporide (100 μM)+DCB (1 μM)+zVAD.FMK(200 μM)	+	+	34** (1.9)	47** (2.8)				
Cariporide (100 μM)+SEA400 (1 μM)	+	+	15* (3.0)	82* (4.5)	17* (3.5)	69* (2.6)	25* (3.6)	77* (3.1)
Cariporide (100 μM)+SEA400(1 μM)+zVAD.FMK(200 μM)	+	+	18* (3.1)	87* (1.2)	21* (4.4)	87* (1.9)	20* (2.9)	82* (4.2)

This increased intracellular buffering in glioma cells is demonstrated by the higher release of cytosolic free calcium from TG sensitive ER stores and calcium release from FCCP responsive mitochondrial stores. Basally elevated levels of $[Ca^{2+}]_i$ in glioma cells are associated with increased intracel lular buffering as compared with normal astrocytes.

The intracellular release of calcium from ER or mitochon drial stores of U87 glioma cells caused transitory elevations in $[Ca^{2+}]_i$ with restoration to near basal levels within 400 s. Significantly, restoration of basal levels of $[Ca^{2+}]_i$ following TG treatment was prevented by inhibiting sodium dependent calcium efflux (forward mode) by NCX1.1 (Fig. 1, panel A). The whole cell patch recordings of CHO cells transfected with NCX1.1 determined that DCB is a nanomolar inhibitor of the forward mode of NCX1.1 and a micromolar inhibitor of the reverse mode. To our knowledge, this is the first report quantifying these large differences between inhibition of the forward and reverse modes of NCX1.1 by DCB in an intact cell and validated the use of DCB at low concentrations in glioma cells to selectively inhibit the forward mode of NCX1.1. Neither ≤1 μM of DCB nor the use of selective nanomolar inhibitors of the reverse mode of NCX1.1, SEA0400 (Table 1) or KB R79433 (Hegde et al., 2004), evoked glioma cytotoxicity. These pharmacological data coupled with the fura 2 measurements, demonstrated that inhibiting only the forward mode of NCX1.1 was not sufficient to explain the glioma cytotoxicity observed using higher concentrations of either amiloride or DCB (Table 1).

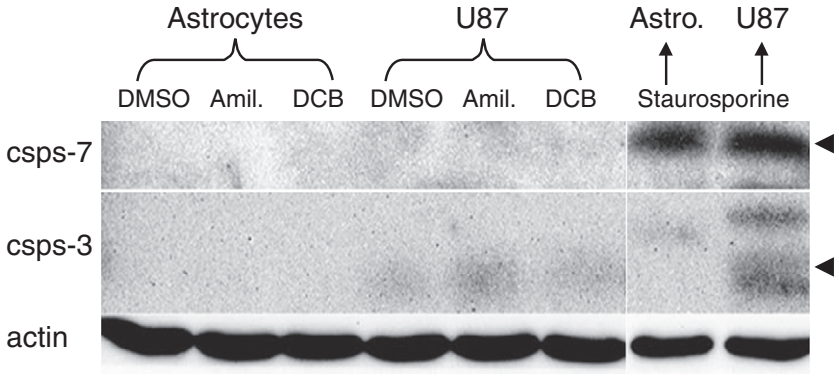

Fig. 5 – Immunoblots of U87 glioma cells and primary astrocytes demonstrate changes in levels of cleaved caspases 3 and 7 (arrowheads) following drug or vehicle (0.1% DMSO) treatments. Staurosporine (10 μM) was included as a positive control to demonstrate caspase activation in glioma cells and astrocytes undergoing apoptosis.

Amiloride is a more potent inhibitor of sodium proton transport (NHE1) than of sodium calcium transport (NCX1.1), but at higher concentrations (≥250 μM) demonstrates inhibition of both transporters (Rogister et al., 2001). Conversely, DCB inhibits NCX1.1 ≫ NHE1, but at higher concentrations (≥20 μM), inhibits both modes of NCX1.1 and NHE1 in U87 glioma cells(Hegde et al., 2004). Consistent with a model comprised of dual inhibition of NCX1.1 and NHE1, low concentration DCB (≤1 μM) inhibits the forward mode of NCX1.1, yet is not cytotoxic to glioma cells until achieving concentrations (≥20 μM) which also inhibit NHE1 (Fig. 1, panel B). Previously we reported that 50 μM of amiloride inhibits NHE1 yet does not kill glioma cells until reaching concentrations that dually inhibit NCX1.1 and NHE1 (Hegde et al., 2004). Employing 1 uM SEA0400 blocked both modes of NCX1.1 and coupled with the NHE1 inhibitor Cariporide, caused glioma cell death while neither agent alone was cytotoxic (Table 1). Analogously, low concentration DCB (1 μM) blocked the forward mode of NCX1.1 and when coupled with Cariporide also triggered cell demise. These drug combinations, like amiloride and 20 μM DCB, were comparably cytotoxic in the presence or absence of pan caspase inhibitors.

Neither the NHE1 inhibitor, Cariporide, or either of the NCX1.1 inhibitors, SEA0400 or DCB (1 μM) were individually cytotoxic to the U87, U251 or U118 human glioma cell lines, which had been previously shown to persistently activate NHE1 and maintain basally elevated pH_i (McLean et al., 2000). However, dual inhibition of NHE1 and NCX1.1 by Cariporide + SEA0400 or Cariporide + DCB (1 μM) was cytotoxic to these glioma cell lines. Dual blockade of NHE1 and NCX1.1 using different inhibitors in the three glioma cell lines demonstrates a consistent pattern of cytotoxic potencies (Table 1). Amiloride or high concentration DCB (20 μM) are consistently more cytotoxic than either Cariporide + SEA0400 or Cariporide + DCB (1 μM). The additional cytotoxicities of amiloride or 20 μM DCB may result from their enhanced inhibitor potencies of the ionic transporters or indicate the possibility of additional drug targeting. Furthermore, amiloride appears to have additional cytostatic activity as its reduction of viable cells exceeds the dead cell counts after 24 h in these glioma cell lines (Table 1).

The caspase independent glioma cell demise triggered by dual inhibition of NHE1 and NCX1.1 is supported by the absence of observed caspase 3 or 7 activation associated with drug treatment. Additionally, the nuclei of these dying glioma cells did not adopt an apoptotic morphology (Fig. 1S). These data support our prior observations that amiloride induced glioma cell death did not activate PARP or Annexin V using FACS analyses (Hegde et al., 2004). Several types of non apoptotic cell death including autophagy and paraptosis have been described that are relevant to cancer therapeutics (Constantinou et al., 2009), and we are currently investigating glioma cell death mechanisms triggered by these agents.

The precise intracellular mechanism(s) by which dual inhibition of NHE1 and NCX1.1 produces selective glioma cell death is unknown at this time. Dual inhibition of NHE1 and NCX1.1 in glioma cells reduces pH_i and could activate ASICs with the increased calcium influx additionally increasing high basal $[Ca^{2+}]_i$. Alternatively, further elevations in calcium release from thapsigargin sensitive ER stores in glioma cells have been reported to activate store operated calcium (SOC) channels that could augment calcium influx and increase $[Ca^{2+}]_i$ to cytotoxic levels when the forward mode of NCX1.1 is inhibited (Kovacs et al., 2005). These pharmacological studies indicate that sodium dependent proton and calcium efflux by ionic transporters assist malignant glioma cells to survive in hypovascularized, acidotic tumor microenvironments and potentially represent important pharmacological targets.

4. Experimental procedures

4.1. *Glioma cell lines and primary astrocyte cultures*

Human U87 and rat C6 glioma cell lines were obtained from the American Tissue Culture Collection. Primary rat astrocytes were isolated from the cerebral cortices of neonatal Sprague Dawley rats (1 2 days old) as described in detail elsewhere (Floyd et al., 2005). Briefly, cortices were cleaned of meninges and white matter, mechanically disseminated, and incubated with papain for 30 min. Astrocyte culture purity was characterized as 98% using GFAP immunocytochemistry as described previously (Amruthesh et al., 1993). Glioma cells and astrocytes were grown on rat tail collagen coated coverslips in DMEM supplemented with 10% fetal bovine serum (Hyclone), 1% L glutamine (200 mM, Gibco), 100 U/ml penicillin and 100 mg/ml streptomycin (Gibco) as detailed in Hegde et al. (2004).

4.2. *Cytosolic free sodium and calcium determinations*

$[Na^+]_i$ and $[Ca^{2+}]_i$ were determined using either SBFI AM or Fura 2 AM, respectively, as described previously (Floyd et al., 2005). Glioma cells were grown on collagen coated coverslips at 37 °C. Cells were washed and then loaded with SBFI AM or Fura 2 AM at RT to control esterase activity and reduce non specific dye uptake by intracellular organelles and then imaged at 37 °C as described in detail elsewhere (Floyd et al., 2005). Cells were rinsed twice and then loaded in HEPES buffered saline with 5 μM Fura 2 AM (60 min) or 20 μM SBFI AM + 0.1% pluronic acid (90 min) at room temperature (20 22 °C) and rinsed before imaging. During the experiments, cells were perfused (flow rate 5 ml/min) with 37 °C HEPES buffered saline and bath temperature monitored and maintained with a Peltier controlled open incubation system (Harvard Apparatus, Holliston, MA).

Intracellular imaging was conducted on a high speed imaging system with excitation light provided by a xenon arc lamp coupled to a Polychrome IV scanning monochromator (Till Photonics, Grafelfing, Germany) that can alternate excitation wavelengths. Excitation light was delivered to cells via fiber optics through the epifluorescence port of a Nikon E600 microscope coupled to a Nikon Fluor 60× water immersion lens. The detector was an Orca II ER CCD digital camera (Hamamatsu USA, Bridgewater, NJ) that is computer controlled by C Imaging SimplePCI software (Compix, Cranberry Township, PA). For *in vitro* ionic measurements, individual cell values from a microscope field (4 7 cells/field) were averaged for each experimental condition. Each experimental condition was repeated a minimum of 3 times totaling 12 21 cells/condition (Floyd et al., 2005).

Calibration of SBFI fluorescent emission to $[Na^+]_i$ was performed using the method described previously (Floyd et al., 2005). Cells were perfused with HR containing 3 μM gramicidin, 100 μM ouabain, and sodium concentrations of 0, 30, or 50 mM. Data were compared to a standard curve generated by perfusing another set of cells with the aforementioned ionophores in the presence of varying buffer containing sodium (0, 10, 30, 50, 70, and 100 mM). Calibration of Fura 2 with $[Ca^{2+}]_i$ utilized the ratiometric method described elsewhere (Grynkiewicz et al., 1985). R_{min} and R_{max} values (340/380 excitation with 505 nM emission) were determined by perfusing cells with HR plus 10 μM ionomycin and either 10 mM EGTA or 5 mM calcium, respectively.

CHO cells stably transfected with NCX1.1 was a kind gift from John Reeves (Reeves and Condrescu, 2003). CHO cells were transfected with the mammalian expression vector pcDNA3 containing the open reading frame for the bovine cardiac Na^+/Ca^{2+} exchanger (NCX1.1; accession number LO6438) with functional recombinants selected using ionomycin. Stable transfectants were maintained in the presence of the antibiotic G418.

4.3. *Measurement of NCX1.1 exchange current*

Whole cell current recordings were performed as described elsewhere (Chen and Yau, 1994) using an Axopatch 200B amplifier. Currents were digitally filtered at 1 kHz and digitized at 2 kHz using Digidata 1320 digitizer and pClamp8 software (Axon Instrument/Molecular Device). Borosilicate glass electrodes were pulled by PP 830 Puller (Narashige Co.), and have a resistance of 1.5 2.0 MΩ when filled with the pipette solution. To record the NCX 1.1 exchanger activity, the clamped whole cell was moved to the mouth of a set of capillary tubes which were controlled by SF 77 solution exchanger (Warner Instruments) and pClamp8 software. The cell was exposed to the control solution and work solution sequentially to monitor the exchanger currents, the clamping potential is 0 mV.

4.3.1. *Forward mode NCX1.1*

For inward sodium current recording, the pipette solution contained (in mM) 120 LiCl, 20 tetramethylammonium chloride (TEA Cl), 5 KCl, 2 $MgCl_2$, 8 D glucose, 10 HEPES, 2 nitrilotriacetic acid (NTA), and 0.346 $CaCl_2$ (20 μM free Ca^{2+}), pH 7.2; the bath control solution contained (in mM) 145 LiCl, 1 $MgCl_2$, 10 D glucose, 10 HEPES, and 1 EGTA, pH 7.4; and the bath work solution contained (in mM) 145 NaCl, 1 $MgCl_2$, 10 D glucose, 10 HEPES, and 1 EGTA, pH 7.4.

4.3.2. *Reverse mode NCX1.1*

For outward current recording, the pipette solution contained (in mM) 120 NaCl, 5 KCl, 2 MgCl, 8 D glucose, 20 tetramethylammonium chloride (TEA Cl), 4.28 $CaCl_2$, 5 EGTA, and 10 HEPES, pH 7.2; the bath control solution contained (in mM) 145 LiCl, 1 $MgCl_2$, 10 D glucose, 0.5 EGTA, and 10 HEPES, pH 7.4; and the bath work solution contained (in mM) 145 LiCl, 1 $MgCl_2$, 10 D glucose, 1 $CaCl_2$, and 10 HEPES, pH 7.4. For inward current recording, the pipette solution contained (in mM) 120 LiCl, 20 TEA Cl, 5 KCl, 2 $MgCl_2$, 8 D glucose, 10 HEPES, 2 nitrilotriacetic acid (NTA), and 0.346 $CaCl_2$ (20 μM free Ca^{2+}), pH 7.2; the bath control solution contained (in mM) 145 LiCl, 1 $MgCl_2$, 10 D glucose, 10 HEPES, and 1 EGTA, pH 7.4; and the bath work solution contained (in mM) 145 NaCl, 1 $MgCl_2$, 10 D glucose, 10 HEPES, and 1 EGTA, pH 7.4.

For drug application, DCB was prepared as stock solutions in DMSO stored at 30 °C. Upon use, the stock solutions were diluted to certain concentrations by bath control or work solutions. To test the drug effects, sodium currents in the absence of drugs were first recorded, and immediately followed by a recording in the presence of certain concentrations of drugs. All experiments were conducted at the room temperature. Data analysis normalized the current under drug treatment conditions to that in the absence of drugs. The normalized value was fitted to a Langmüir function to estimate the half inhibition concentration (IC_{50}). All data points come from the average of 3 5 independent recordings. The data are presented by mean ± standard deviation (SD).

4.4. *Viable cell number and cytotoxicity determination*

96 well plates were initially seeded with 10^4 U87 cells in media described earlier and allowed to adhere for 24 h. Stock drug concentrations were dissolved in DMSO and added to the media with a final vehicle concentration of 0.1% DMSO. Following treatment, 10 μl of water soluble tetrazolium (10% v/v, WST, Roche) was added, the plate shaken for 5 s, and read on a plate reader 3 h after the addition of tetrazolium dye. Viable cell numbers, measured as absorbance values, were normalized using control curve determined for each cell type. Cells were removed by gentle rinsing with PBS following absorbance determinations. Trypan blue was added to cell suspension (10% v/v) and after 5 min an aliquot was transferred to a manual hemacytometer for cell counting.

4.5. *Nuclear morphology cell death studies*

Treated and stage matched, vehicle treated cells were evaluated for cell death in the presence of zVAD FMK (20 μM), a pan caspase inhibitor, and the results were averaged from at least six experiments. The nuclei of treated and untreated glioma cells were stained with 10 μM Hoechst 33342 (Sigma) for 30 min and visualized on a Nikon E600 fluorescent microscope.

4.6. *Immunoblotting*

Cells in six well plates were lysed with 300 μl Laemmli buffer (0.03 M Tris HCl, 0.02% SDS, 0.5 M β mercaptoethanol, 7% glycerol, and 0.01% bromophenol blue) and boiled for 10 min at 90 °C. The lysates were fractionated by molecular weight using dodecyl sulfate polyacrylamide gel electrophoresis, transferred to nitrocellulose (Bio Rad Laboratories), blocked for 1 h in TBS Triton containing 5% dried milk, and blotted with the antibodies indicated in the figures. Horseradish peroxidase conjugated secondary antibodies and SuperSignal detection reagents (West Femto and West Pico from Pierce and Thermo Scientific, respectively) were used for detection, and chemiluminescent images were captured using an Alpha Innotech imaging station. Mouse anti β actin AC 15 was purchased from Sigma. Rabbit anti cleaved caspase 3 and rabbit anti cleaved caspase 7 were purchased from Cell Signaling

Technologies. Horseradish peroxidase conjugated goat anti mouse IgG and horseradish peroxidase conjugated goat anti rabbit IgG were from Zymed and Pierce, respectively.

4.7. *Statistical analysis*

Data in Table 1 are presented as mean ± standard error of the mean (SEM). Statistical significance was determined for cell number and cytotoxicity using one way analysis of variance and Bonferroni's test for multiple pairwise comparisons using SigmaStat software version 2.00 (SPSS Science Inc, Chicago, IL).

Supplementary materials related to this article can be found online at doi: 10.1016/j.brainres.2010.09.059.

Role of funding sources

This research funded by the National Institutes of Health (NS040489, NS060880 F.G., and NS045136 B.L.).

Conflict of interest

Fredric Gorin, Michael Nantz, and the University of California have filed patents pertaining to the use of amiloride and novel derivatives as potential anti cancer agents. Fredric Gorin is CEO of D3G, which contracts with publically owned and private labs to perform pre clinical drug discovery, as it pertains to advance the treatment of primary and metastatic cancers affecting the central nervous system (brain and spinal cord).

Acknowledgments

SEA0400 was a kind gift from Professor Baba, Department of Pharmacology, Graduate School of Pharmaceutical Sciences, University of Shizuoka, Japan.

REFERENCES

Amoroso, S., De Maio, M., Russo, G.M., Catalano, A., Bassi, A., Montagnani, S., Renzo, G.D., Annunziato, L., 1997. Pharmacological evidence that the activation of the Na(+) Ca2+ exchanger protects C6 glioma cells during chemical hypoxia. Br. J. Pharmacol. 121, 303 309.

Amruthesh, S.C., Boerschel, M.F., McKinney, J.S., Willoughby, K.A., Ellis, E.F., 1993. Metabolism of arachidonic acid to epoxyeicosatrienoic acids, hydroxyeicosatetraenoic acids, and prostaglandins in cultured rat hippocampal astrocytes. J. Neurochem. 61, 150 159.

Barker II, F.G., Davis, R.L., Chang, S.M., Prados, M.D., 1996. Necrosis as a prognostic factor in glioblastoma multiforme. Cancer 77, 1161 1166.

Brandes, A.A., Vastola, F., Monfardini, S., 1999. Reoperation in recurrent high grade gliomas: literature review of prognostic factors and outcome. Am. J. Clin. Oncol. 22, 387 390.

Chalmers, S., Nicholls, D.G., 2003. The relationship between free and total calcium concentrations in the matrix of liver and brain mitochondria. J. Biol. Chem. 278, 19062 19070.

Chamberlain, M.C., Johnston, S.K., 2010. Salvage therapy with single agent bevacizumab for recurrent glioblastoma. J. Neurooncol. 96 (2), 259 269.

Chen, T.Y., Yau, K.W., 1994. Direct modulation by Ca(2+) calmodulin of cyclic nucleotide activated channel of rat olfactory receptor neurons. Nature 368, 545 548.

Compostella, A., Tosoni, A., Blatt, V., Franceschi, E., Brandes, A.A., 2007. Prognostic factors for anaplastic astrocytomas. J. Neurooncol. 81, 295 303.

Constantinou, C., Papas, K.A., Constantinou, A.I., 2009. Caspase independent pathways of programmed cell death: the unraveling of new targets of cancer therapy? Curr. Cancer Drug Targets 9, 717 728.

Deitmer, J.W., Broer, A., Broer, S., 2003. Glutamine efflux from astrocytes is mediated by multiple pathways. J. Neurochem. 87, 127 135.

Dinca, E.B., Sarkaria, J.N., Schroeder, M.A., Carlson, B.L., Voicu, R., Gupta, N., Berger, M.S., James, C.D., 2007. Bioluminescence monitoring of intracranial glioblastoma xenograft: response to primary and salvage temozolomide therapy. J. Neurosurg. 107, 610 616.

Ducret, T., Vacher, A.M., Vacher, P., 2003. Voltage dependent ionic conductances in the human malignant astrocytoma cell line U87 MG. Mol. Membr. Biol. 20, 329 343.

Erecinska, M., Nelson, D., Dagani, F., Deas, J., Silver, I.A., 1993. Relations between intracellular ions and energy metabolism under acidotic conditions: a study with nigericin in synaptosomes, neurons, and C6 glioma cells. J. Neurochem. 61, 1356 1368.

Floyd, C.L., Gorin, F.A., Lyeth, B.G., 2005. Mechanical strain injury increases intracellular sodium and reverses Na+/Ca2+ exchange in cortical astrocytes. Glia 51, 35 46.

Galiano, M., Gasparre, G., Lippe, C., Cassano, G., 2004. Inositol 1, 4, 5 trisphosphate and ryanodine receptors mobilize calcium from a common functional pool in human U373 MG cells. Cell Calcium 36, 359 365.

Goldman, W.F., Yarowsky, P.J., Juhaszova, M., Krueger, B.K., Blaustein, M.P., 1994. Sodium/calcium exchange in rat cortical astrocytes. J. Neurosci. 14, 5834 5843.

Gorin, F., Harley, W., Schnier, J., Lyeth, B., Jue, T., 2004. Perinecrotic glioma proliferation and metabolic profile within an intracerebral tumor xenograft. Acta Neuropathol. 107, 235 244.

Gorin, F.a.N., M., 2007. Amino acid and peptide conjugates of amiloride and methods of use thereof. Vol., USPTO, ed., USA.

Griguer, C.E., Oliva, C.R., Gillespie, G.Y., 2005. Glucose metabolism heterogeneity in human and mouse malignant glioma cell lines. J. Neurooncol. 74, 123 133.

Grynkiewicz, G., Poenie, M., Tsien, R.Y., 1985. A new generation of Ca2+ indicators with greatly improved fluorescence properties. J. Biol. Chem. 260, 3440 3450.

Handfield Jones, S., Jones, S., Peachey, R., 1988. High dose nicotinamide in the treatment of necrobiosis lipoidica. Br. J. Dermatol. 118, 693 696.

Hartmann, J., Verkhratsky, A., 1998. Relations between intracellular Ca2+ stores and store operated Ca2+ entry in primary cultured human glioblastoma cells. J. Physiol. 513 (Pt 2), 411 424.

Hegde, M., Roscoe, J., Cala, P., Gorin, F., 2004. Amiloride kills malignant glioma cells independent of its inhibition of the sodium hydrogen exchanger. J. Pharmacol. Exp. Ther. 310, 67 74.

Ishiuchi, S., Yoshida, Y., Sugawara, K., Aihara, M., Ohtani, T., Watanabe, T., Saito, N., Tsuzuki, K., Okado, H., Miwa, A., Nakazato, Y., Ozawa, S., 2007. Ca2+ permeable AMPA receptors regulate growth of human glioblastoma via Akt activation. J. Neurosci. 27, 7987 8001.

Iwamoto, T., 2004. Forefront of Na+/Ca2+ exchanger studies: molecular pharmacology of Na+/Ca2+ exchange inhibitors. J. Pharmacol. Sci. 96, 27 32.

Kahlert, S., Schild, L., Reiser, G., 2001. Mitochondrial polarization in rat hippocampal astrocytes is resistant to cytosolic Ca(2+) loads. J. Neurosci. Res. 66, 1019 1027.

Korkolopoulou, P., Perdiki, M., Thymara, I., Boviatsis, E., Agrogiannis, G., Kotsiakis, X., Angelidakis, D., Rologis, D., Diamantopoulou, K., Thomas Tsagli, E., Kaklamanis, L., Gatter, K., Patsouris, E., 2007. Expression of hypoxia related tissue factors in astrocytic gliomas. A multivariate survival study with emphasis upon carbonic anhydrase IX. Hum. Pathol. 38, 629 638.

Kovacs, G.G., Zsembery, A., Anderson, S.J., Komlosi, P., Gillespie, G.Y., Bell, P.D., Benos, D.J., Fuller, C.M., 2005. Changes in intracellular Ca2+ and pH in response to thapsigargin in human glioblastoma cells and normal astrocytes. Am. J. Physiol. Cell Physiol. 289, C361 C371.

Kwan, D.H., Kam, A.Y., Wong, Y.H., 2008. Activation of the human FPRL 1 receptor promotes Ca2+ mobilization in U87 astrocytoma cells. Neurochem. Res. 33, 125 133.

Lamszus, K., Kunkel, P., Westphal, M., 2003. Invasion as limitation to anti angiogenic glioma therapy. Acta Neurochir. Suppl. 88, 169 177.

Lee, C., Visen, N.S., Dhalla, N.S., Le, H.D., Isaac, M., Choptiany, P., Gross, G., Omelchenko, A., Matsuda, T., Baba, A., Takahashi, K., Hnatowich, M., Hryshko, L.V., 2004. Inhibitory profile of SEA0400 [2 [4 [(2, 5 difluorophenyl)methoxy]phenoxy] 5 ethoxyaniline] assessed on the cardiac Na+ Ca2+ exchanger, NCX1.1. J. Pharmacol. Exp. Ther. 311, 748 757.

Legler, J.M., Ries, L.A., Smith, M.A., Warren, J.L., Heineman, E.F., Kaplan, R.S., Linet, M.S., 1999. Cancer surveillance series [corrected]: brain and other central nervous system cancers: recent trends in incidence and mortality. J. Natl Cancer Inst. 91, 1382 1390.

Maintz, D., Heindel, W., Kugel, H., Jaeger, R., Lackner, K.J., 2002. Phosphorus 31 MR spectroscopy of normal adult human brain and brain tumours. NMR Biomed. 15, 18 27.

Masereel, B., Pochet, L., Laeckmann, D., 2003. An overview of inhibitors of Na(+)/H(+) exchanger. Eur. J. Med. Chem. 38, 547 554.

McLean, L.A., Roscoe, J., Jorgensen, N.K., Gorin, F.A., Cala, P.M., 2000. Malignant gliomas display altered pH regulation by NHE1 compared with nontransformed astrocytes. Am. J. Physiol. Cell Physiol. 278, C676 C688.

Page, A.J., Brierley, S.M., Martin, C.M., Hughes, P.A., Blackshaw, L.A., 2007. Acid sensing ion channels 2 and 3 are required for inhibition of visceral nociceptors by benzamil. Pain 133, 150 160.

Perez Velazquez, J.L., Frantseva, M., Naus, C.C., Bechberger, J.F., Juneja, S.C., Velumian, A., Carlen, P.L., Kidder, G.M., Mills, L.R., 1996. Development of astrocytes and neurons in cultured brain slices from mice lacking connexin43. Brain Res. Dev. Brain Res. 97, 293 296.

Reeves, J.P., Condrescu, M., 2003. Allosteric activation of sodium calcium exchange activity by calcium: persistence at low calcium concentrations. J. Gen. Physiol. 122, 621 639.

Reichert, M., Steinbach, J.P., Supra, P., Weller, M., 2002. Modulation of growth and radiochemosensitivity of human malignant glioma cells by acidosis. Cancer 95, 1113 1119.

Rogister, F., Laeckmann, D., Plasman, P., Van Eylen, F., Ghyoot, M., Maggetto, C., Liegeois, J., Geczy, J., Herchuelz, A., Delarge, J., Masereel, B., 2001. Novel inhibitors of the sodium calcium exchanger: benzene ring analogues of N guanidino substituted amiloride derivatives. Eur. J. Med. Chem. 36, 597 614.

Schnier, J.B., Nishi, K., Harley, W.R., Gorin, F.A., 2008. An acidic environment changes cyclin D1 localization and alters colony forming ability in gliomas. J. Neurooncol. 89, 19 26.

Spassova, M.A., Soboloff, J., He, L.P., Hewavitharana, T., Xu, W., Venkatachalam, K., van Rossum, D.B., Patterson, R.L., Gill, D.L., 2004. Calcium entry mediated by SOCs and TRP channels: variations and enigma. Biochim. Biophys. Acta 1742, 9 20.

Tannock, I.F., Rotin, D., 1989. Acid pH in tumors and its potential for therapeutic exploitation. Cancer Res. 49, 4373 4384.

Vali, S., Carlsen, R., Pessah, I., Gorin, F., 2000. Role of the sarcoplasmic reticulum in regulating the activity dependent expression of the glycogen phosphorylase gene in contractile skeletal muscle cells. J. Cell. Physiol. 185, 184 199.

Vaupel, P., Mayer, A., 2007. Hypoxia in cancer: significance and impact on clinical outcome. Cancer Metastasis Rev. 26, 225 239.

Vila Carriles, W.H., Kovacs, G.G., Jovov, B., Zhou, Z.H., Pahwa, A.K., Colby, G., Esimai, O., Gillespie, G.Y., Mapstone, T B., Markert, J.M., Fuller, C.M., Bubien, J.K., Benos, D.J., 2006. Surface expression of ASIC2 inhibits the amiloride sensitive current and migration of glioma cells. J. Biol. Chem. 281, 19220 19232.

Wang, J., Zhang, Z., Hu, Y., Hou, X., Cui, Q., Zang, Y., Wang, C., 2007. SEA0400, a novel Na+/Ca2+ exchanger inhibitor, reduces calcium overload induced by ischemia and reperfusion in mouse ventricular myocytes. Physiol. Res. 56, 17 23.

Wu, M., Neilson, A., Swift, A.L., Moran, R., Tamagnine, J., Parslow, D., Armistead, S., Lemire, K., Orrell, J., Teich, J., Chomicz, S., Ferrick, D.A., 2007. Multiparameter metabolic analysis reveals a close link between attenuated mitochondrial bioenergetic function and enhanced glycolysis dependency in human tumor cells. Am. J. Physiol. Cell Physiol. 292, C125 C136.